

Non-linear and non-empirical double hybrid density functional

Danish Khan*

*Chemical Physics Theory Group, Department of Chemistry, University of Toronto,
St. George Campus, Toronto, ON, Canada and
Vector Institute for Artificial Intelligence, Toronto, ON, M5S 1M1, Canada*

We develop a non-linear and non-empirical (nLanE) double hybrid density functional derived from an accurate interpolation of the adiabatic connection in density functional theory, incorporating the correct asymptotic expansions. By bridging the second-order perturbative weak correlation limit with the fully interacting limit from the semi-local SCAN functional, nLanE-SCAN is free of fitted parameters while providing improved energetic predictions compared to SCAN for moderately and strongly correlated systems alike. It delivers accurate predictions for atomic total energies and multiple reaction datasets from the GMTKN55 benchmark while significantly outperforming traditional linear hybrids and double hybrids for non-covalent interactions without requiring dispersion corrections. Due to the exact constraints at the weak correlation limit, nLanE-SCAN has reduced delocalization errors as evident through SIE4x4 and bond dissociations of H_2^+ and He_2^+ . Its proper asymptotic behavior ensures stability in strongly correlated systems, improving H_2 and N_2 bond dissociation profiles compared to conventional functionals.

Kohn-Sham (KS) density functional theory (DFT), the workhorse of computational simulations in chemistry and materials science [1, 2], only requires the exchange-correlation (XC) energy to be approximated as a functional of the density/orbitals [3]. The adiabatic connection (AC) formalism [4–6] is a general, powerful tool for the development of XC functionals. For several decades it has been used to justify the introduction of hybrid [7–9] and double hybrid (DH) functionals [10–12] and successively it has been directly employed to construct high-level XC functionals based on AC models (ACM) interpolating between known limits of the AC integrand [13–18].

The XC functionals based on ACMs have the general form

$$E_{\text{xc}}^{\text{ACM}} = f^{\text{ACM}}(\mathbf{W}) = \int_0^1 W_\lambda^{\text{ACM}}(\mathbf{W}) d\lambda \quad (1)$$

where $\mathbf{W} = (W_0, W'_0, W_\infty, W'_\infty)$, with $W_0 = E_{\text{x}}^{\text{HF}}$ being the Hartree-Fock (exact) exchange energy on the Kohn-Sham (KS) orbitals, $W'_0 = 2E_{\text{c}}^{\text{GL2}}$ being twice the correlation energy from second-order Görling-Levy (GL) perturbation theory [19], and W_∞ and W'_∞ being the indirect part of the minimum expectation value of the electron-electron repulsion for a given density and the potential energy of coupled zero-point oscillations around this minimum, respectively [15, 20]. The model W_λ^{ACM} is designed to mimic the exact but unknown W_λ , in particular by considering the known asymptotic expansions [15, 19–21]

$$W_{\lambda \rightarrow 0} = E_{\text{x}}^{\text{HF}} + \sum_{n=2}^{\infty} n E_{\text{c}}^{\text{GLn}} \lambda^{n-1} \quad (2)$$

$$W_{\lambda \rightarrow \infty} = W_\infty + W'_\infty \lambda^{-1/2} + W''_\infty \lambda^{-3/2} + \mathcal{O}(\lambda^{-5/2}) \quad (3)$$

Functionals constructed in such a way perform remarkably well for strongly correlated systems but can be rather

inaccurate for general main-group thermochemistry and kinetics [22] where standard density functional approximations (DFAs) excel. In this work we will derive a functional that incorporates information from the fully interacting physical limit of the adiabatic connection, i.e. $\lambda = 1$, rather than the $\lambda \rightarrow \infty$ limit. Hence, the ingredients used within our functional correspond to $\mathbf{W} = (W_0, W'_0, W_1)$. The $\lambda \rightarrow \infty$ asymptotic behaviour from eq. (3) will be incorporated implicitly through the chosen form of the function W_λ . For this we modify the [1,1] Padé form proposed by Ernzerhof [23] to

$$W_\lambda = a + \frac{b\sqrt{\lambda+1}}{c\lambda+1} \quad (4)$$

where a , b , c are density/orbital dependent quantities to be evaluated through the constraints based on $\mathbf{W} = (W_0, W'_0, W_1)$. Eq. (4) inherits the required smoothness and convexity properties [15] of the original Padé form, while correcting the $\lambda \rightarrow \infty$ asymptotic expansion similar to eq. 3

$$W_{\lambda \rightarrow \infty} = a + \frac{b}{c} \lambda^{-1/2} + \frac{b(c-2)}{2c^2} \lambda^{-3/2} + \mathcal{O}(\lambda^{-5/2}) \quad (5)$$

For calculating a , b , c we impose the following three exact or approximate constraints

$$W_0 = E_{\text{x}}^{\text{HF}} \implies a + b = E_{\text{x}}^{\text{HF}} \quad (6)$$

$$W'_0 = 2E_{\text{c}}^{\text{GL2}} \approx 2E_{\text{c}}^{\text{MP2}} \implies b\left(\frac{1}{2} - c\right) = 2E_{\text{c}}^{\text{MP2}} \quad (7)$$

$$W_1 \approx W_1^{\text{SCAN}} \implies a + \frac{b\sqrt{2}}{c+1} = W_1^{\text{SCAN}} \quad (8)$$

where $E_{\text{c}}^{\text{MP2}}$ denotes the correlation energy from second-order Møller-Plesset (MP) perturbation theory

on the KS occupied (occ.) and virtual (virt.) orbitals with eigenvalues ε

$$E_c^{\text{MP2}} = -\frac{1}{4} \sum_{ab}^{\text{virt.}} \sum_{ij}^{\text{occ.}} \frac{|\langle ab|\hat{v}_{ee}|ij\rangle - \langle ab|\hat{v}_{ee}|ji\rangle|^2}{\varepsilon_a + \varepsilon_b - \varepsilon_i - \varepsilon_j} \quad (9)$$

with \hat{v}_{ee} denoting the electron repulsion operator. The first two constraints (eqs. 6, 7) can be generalized to match higher order Taylor expansion of the interpolating function (eq. 4) with exact values from perturbation theory (eq. 2) at $\lambda = 0$. For instance, an additive parameter d in the denominator of eq. 4 would still preserve the correct asymptotic expansion (eq. 3) and this can be used to add an additional constraint incorporating the GL3 (or MP3) energy as

$$W_0'' = 6E_c^{\text{GL3}} \quad (10)$$

In the current work we restrict ourselves to the MP2 term in eq. 7 for computational efficiency.

Eq. 7 contains an error due to the approximation made by ignoring the single-excitation term within the GL2 energy

$$E_c^{\text{GL2}} = E_c^{\text{MP2}} - \sum_a^{\text{virt}} \sum_i^{\text{occ}} \frac{|\langle a|\hat{v}_x^{\text{KS}} - \hat{v}_x^{\text{HF}}|i\rangle|^2}{\varepsilon_a - \varepsilon_i} \quad (11)$$

where \hat{v}_x^{KS} , \hat{v}_x^{HF} denote the local and non-local KS, HF exchange operators respectively. Note that conventional linear double hybrid functionals compensate for this error through empirical fitting [24], but this error remains uncorrected within our functional. Eq. 6 and eq. 7 incorporate (near) exact values using wavefunction theory from the weak correlation limit of the AC within our functional. This is important since semi-local functionals are least accurate in this regime due to greater delocalization of the XC-hole. For the third constraint (eq. 8), we incorporate information from the, unknown, fully-interacting $\lambda = 1$ limit of the physical system where semi-local functionals are much more accurate due to more localized XC-holes [25]. This limit is estimated in our work using the highly accurate strongly constrained and appropriately normed (SCAN) semi-local functional, derived by imposing 17 exact constraints of the universal functional, and normed for cases where semi-local functionals should be accurate [25].

The W_λ value at any arbitrary scaling λ can be calculated for a semi-local DFA using the Levy-Perdew scaling relation[29]

$$W_\lambda^{\text{DFA}}[\rho] = E_x^{\text{DFA}}[\rho] + 2E_c^{\text{DFA}}[\rho_{1/\lambda}]\lambda + \frac{\partial E_c^{\text{DFA}}[\rho_{1/\lambda}]}{\partial \lambda} \lambda^2 \quad (12)$$

with $\rho_{1/\lambda}(\mathbf{r}) = \lambda^{-3}\rho(\mathbf{r}/\lambda)$ being the coordinate-scaled[30, 31] density. This form simplifies at the physical limit $\lambda = 1$

$$W_1^{\text{DFA}}[\rho] = E_x^{\text{DFA}}[\rho] + 2E_c^{\text{DFA}}[\rho] + \frac{\partial E_c^{\text{DFA}}[\rho_{1/\lambda}]}{\partial \lambda} \Big|_{\lambda=1} \quad (13)$$

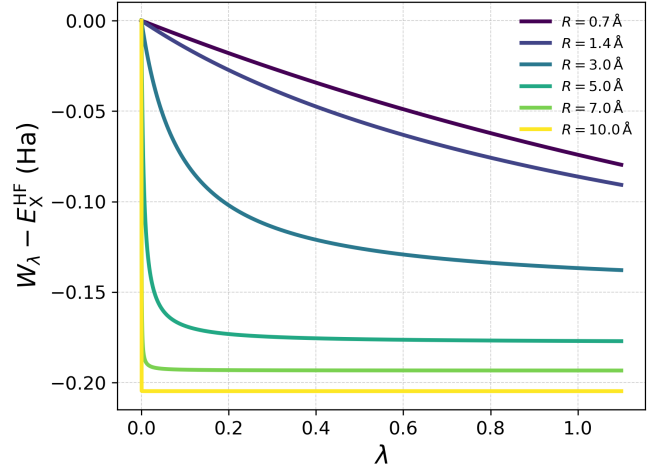


FIG. 1. nLanE-SCAN's (correlation) adiabatic connection curves for the H_2 molecule at different bond-lengths R . The curves plot eq. 4 with the W_0, W_0', W_1 values from eqs. 6, 7, 8 as constraints for obtaining a, b, c . See figure 8 in Ref. [18] for the corresponding exact (Full-CI) adiabatic connection curves.

For simplicity, in our work we ignore the derivative term in this expression (this holds in the low-density limit) and use the following approximation in the third constraint (eq. 8)

$$W_1 \approx W_1^{\text{SCAN}} \approx E_x^{\text{SCAN}} + 2E_c^{\text{SCAN}} \quad (14)$$

with $E_x^{\text{SCAN}}, 2E_c^{\text{SCAN}}$ denoting the exchange and correlation energies from the SCAN functional respectively. This approximation is another source of error within our functional which will be analyzed/fixed through automatic differentiation techniques [32] or empirical fitting in future work.

The three equations in eqs. 6, 7, 8 can be solved analytically (eq. 16) and applying the definition of the adiabatic connection provides a closed form expression for this non-linear and non-empirical (nLanE) double hybrid density functional approximation

$$E_{\text{xc}}^{\text{nLanE}} = \int_0^1 W_\lambda d\lambda$$

$$E_{\text{xc}}^{\text{nLanE}} = \frac{4E_c^{\text{MP2}}}{0.5c - c^2} \left(\sqrt{2} - 1 + \sqrt{\frac{1-c}{c}} \left[\arctan \left(\sqrt{\frac{c}{1-c}} \right) - \arctan \left(\sqrt{\frac{2c}{1-c}} \right) \right] - \frac{c}{2} \right) + E_x^{\text{HF}} \quad (15)$$

where

$$c = \frac{\sqrt{9\alpha^2 - 16\sqrt{2}\alpha + 12\alpha + 4} - \alpha + 2}{4\alpha},$$

$$\alpha = \frac{E_x^{\text{SCAN}} - E_x^{\text{HF}} + 2E_c^{\text{SCAN}}}{2E_c^{\text{MP2}}} \quad (16)$$

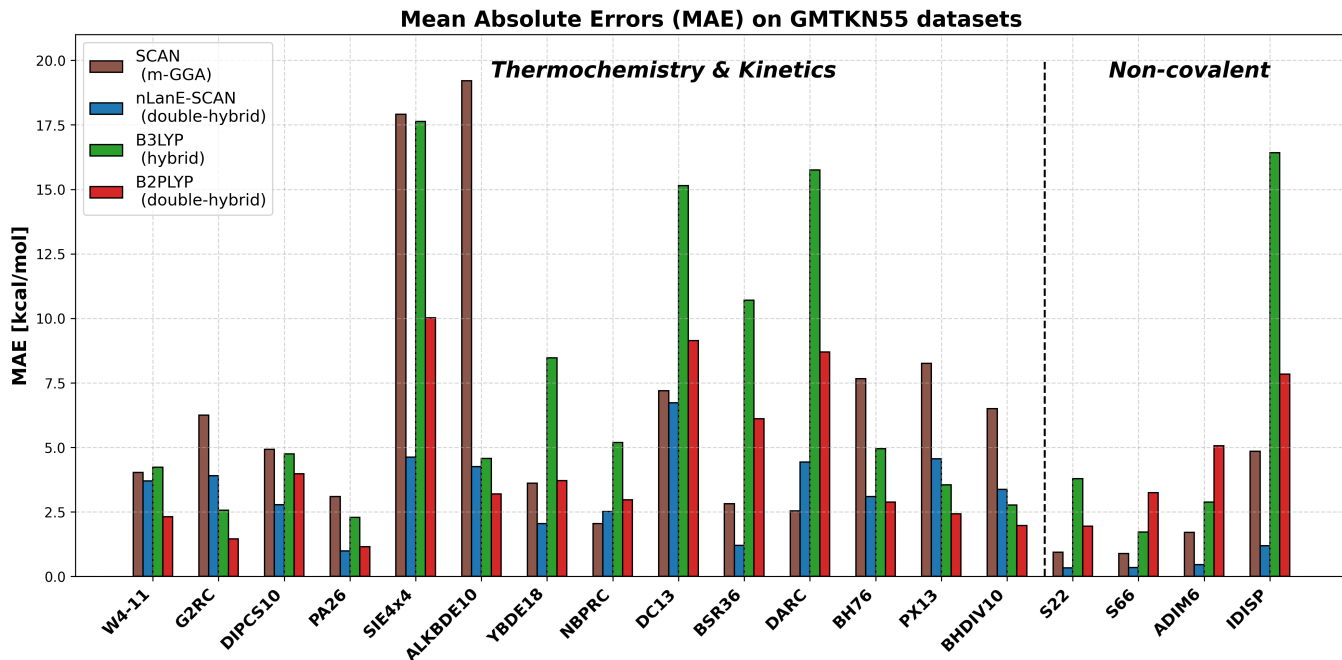


FIG. 2. Mean absolute errors across 18 datasets of (mostly) small molecules from the GMTKN55 benchmark [26]. Errors for the SCAN, B3LYP, B2PLYP functionals are taken from the GMTKN55 paper. All nLanE-SCAN results are using SCAN orbitals. See Data and code availability section below for code to re-produce these results. See Table II in Appendix below for the nLanE-SCAN MAE values plotted in this figure.

Note that the expression in eq. 15 is independent of the choice of semi-local DFA for the W_1 limit in eq. 14 which is only present in the α ratio in eq. 16. Due to our use of SCAN in eq. 14 in the current work, all our results are denoted as nLanE-SCAN. Hence, eq. 15 fixes the weak correlation limit of SCAN’s adiabatic connection through (near) exact values (upto second-order) while retaining the correlated-limit of SCAN. Furthermore, the interpolation is made using a function (eq. 4) that satisfies all known requirements of the adiabatic connection. This

Atom	Exact	SCAN	nLanE-SCAN	B3LYP	B2PLYP
H	-0.500	-0.500	-0.500	-0.499	-0.499
He	-2.904	-2.905	-2.904	-2.908	-2.904
Li	-7.478	-7.480	-7.474	-7.482	-7.474
Be	-14.667	-14.650	-14.657	-14.659	-14.655
B	-24.654	-24.641	-24.646	-24.647	-24.643
C	-37.845	-37.839	-37.841	-37.839	-37.837
N	-54.589	-54.589	-54.588	-54.580	-54.581
O	-75.067	-75.072	-75.066	-75.069	-75.066
F	-99.734	-99.745	-99.733	-99.739	-99.736
Ne	-128.939	-128.947	-128.936	-128.937	-128.938
MAE (kcal/mol)	-	3.95	2.14	3.06	3.13

TABLE I. Total atomic energies (in Hartree) for the first 10 chemical elements compared to exact values from Refs. [7, 33]. Last row shows the mean absolute error (MAE) in kcal/mol. All nLanE-SCAN results are using SCAN orbitals.

is likely the reason why nLanE-SCAN improves upon SCAN in virtually all cases as shown in our results below,

without using any empirical fitting.

Eq. 15 must be contrasted to traditional, linear (double) hybrid functionals

$$E_{xc}^{(\text{double}) \text{ hybrid}} = \xi_1 E_x^{\text{HF}} + \xi_2 E_c^{\text{MP2}} + \xi_3 E_x^{\text{DFA}} + \xi_4 E_c^{\text{DFA}} \quad (17)$$

where $\xi_1, \xi_2, \xi_3, \xi_4$ are scaling parameters usually obtained through empirical fitting. Note that often $\xi_3 = 1 - \xi_1$ and $\xi_4 = 1 - \xi_2$ thereby making ξ_1, ξ_2 ”mixing-fractions” of HF-exchange and MP2 correlation energy respectively. Eq. 15 does not have a concept of such mixing fractions since HF-exchange and MP2-correlation enter through the matching of the Taylor series of our interpolant for the AC (eq. 6, eq. 7) with exact values from perturbation theory at $\lambda = 0$. Hence, nLanE still reduces delocalization errors, as demonstrated through our results below, without the use of such ”mixing-fractions”. For comparison, we include the two most popular (empirical) linear hybrid and double hybrid functionals, namely B3LYP [7] and B2PLYP [34] respectively in all our subsequent results.

A major drawback of ACM functionals such as nLanE is the lack of size-consistency which linear double hybrids do not suffer from. The size consistency is, however, straightforward to restore at no additional cost [35]. We note that none of our subsequent results with nLanE-SCAN have been corrected for the size-consistency error since these were found to be nearly negligible in most

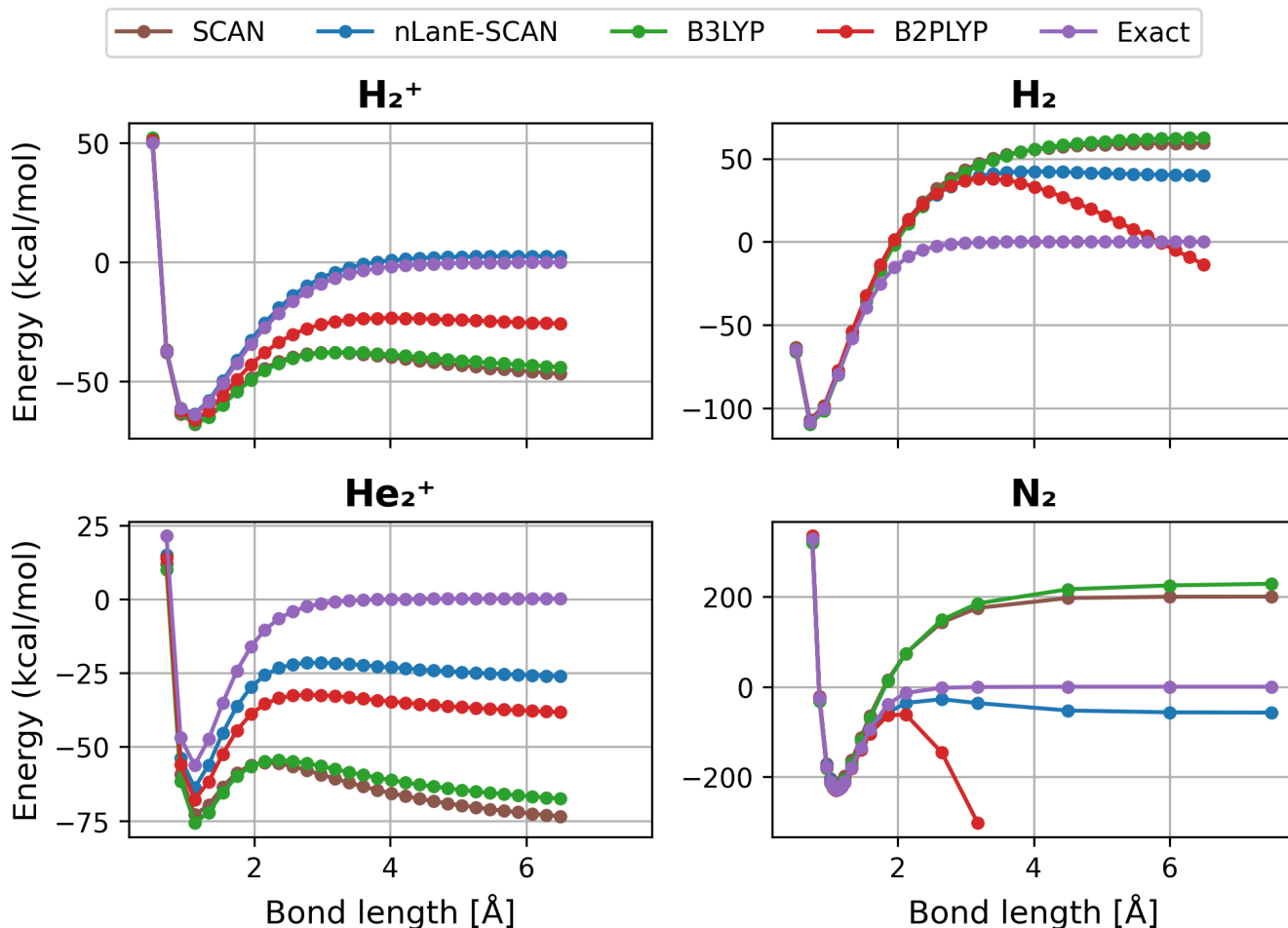


FIG. 3. Bond dissociation curves for four diatomic molecules. Unrestricted calculations were used for the open-shell species (H_2^+ and He_2^+), while restricted calculations were performed for H_2 and N_2 . The "Exact" reference corresponds to all-electron CCSD(T) results for all systems except N_2 , where we use the accurate r_{12} -MR-ACPF values reported in Table 2 of Ref. [27]. All DFT and CCSD(T) calculations employed the cc-pVQZ basis set [28]. All nLanE-SCAN results are using SCAN orbitals.

cases. This will be analyzed more thoroughly in a follow-up work.

We briefly describe the computational details for our results. All results reported with nLanE-SCAN in this work are based on SCAN orbitals, i.e. not self-consistent. The proper terminology would then be nLanE-SCAN@SCAN but we suppress the notation for the orbitals throughout. Following a self-consistent SCAN calculation, E_x^{HF} and E_c^{MP2} (all electron) energies are calculated on these orbitals and the value from eq. 15 is used to replace the SCAN XC-energy. PySCF 2.8.0 has been used to generate all results [36] and the code for this non self-consistent nLanE energy calculation (with any choice of DFA for the orbitals and W_1 limit) is publicly available on GitHub (github.com/dkhan42/nLanE-DH). Unless stated otherwise, the def2-QZVPP basis set [37] was used in all our calculations. Other basis sets, as suggested in Ref. [38], maybe useful due to the slow convergence of MP2 correlation energies. No density-fitting has

been employed in our current nLanE-SCAN results but the option to use density-fitting for the SCF and MP2 is available in our code. A fully self-consistent nLanE implementation using the optimized effective potential [39] based implementation in Ref. [40] will be provided in a follow-up work.

Table I shows the total atomic energy comparison of nLanE-SCAN with SCAN, B3LYP and B2PLYP functionals. The exact values for comparison are taken from Refs. [7, 33] which were used in the optimization of the 3 parameters within the B3LYP linear hybrid. nLanE-SCAN shows the lowest average error for these atomic energies, improving the energy predictions of SCAN and nearly halving the overall average error without any fitted parameters.

The robustness of nLanE for general chemical predictions is tested on datasets from the diverse GMTKN55 benchmark dealing with thermochemistry, kinetics and non-covalent interactions for molecular systems composed of

main-group elements [26]. Figure 2 shows the mean absolute errors (MAE) on 18 datasets (mostly smaller systems) of the GMTKN55 benchmark covering the three aforementioned categories for the SCAN, B3LYP, B2PLYP and nLanE-SCAN functionals. We note here that the nLanE double hybrid has no parameters and was not fitted to any atomic or molecular system. This is in contrast to the B3LYP and B2PLYP functionals which were fitted to molecules and reactions from a few of the subsets (e.g. G2RC and BH76) shown in figure 2. Despite this, nLanE-SCAN either outperforms or matches closely the performance of these empirical functionals across all shown datasets. Furthermore, nLanE-SCAN improves the predictions from SCAN across 16 out of the 18 datasets, a few quite significantly such as SIE4x4 and ALKBDE10 where the average error is reduced by more than 10 kcal/mol. The SIE4x4 dataset in particular deals with systems with large delocalization errors which plague all DFAs. Accurate predictions on this dataset generally require large fractions of HF exchange within traditional linear hybrids, for e.g. in Ref. [41] a SCAN (r²SCAN [42]) based hybrid with 50 % HF exchange and empirical dispersion corrections was shown to achieve an error of 4.6 kcal/mol on this dataset. This fraction, however, is not optimal for most other datasets where 25 % HF exchange was found to be generally more accurate. nLanE-SCAN achieves a similar error of 4.62 kcal/mol on SIE4x4 without any tuning, significantly better than both B3LYP and B2PLYP, and without the concept of HF exchange mixing fractions. It is also generally superior to the B2PLYP double hybrid for all tasks other than barrier heights (BH76, PX13, BHDIV10 datasets). On the non-covalent interaction datasets in particular, nLanE-SCAN improves upon the semi-local SCAN functional which captures mid-range dispersion interactions, outperforming both the B3LYP and B2PLYP non-local functionals. This is a general quality of ACM based functionals which has been noted earlier [43].

Figure 3 shows bond-dissociation plots for 2 charged and 2 neutral diatomics. Across all 4 cases, nLanE-SCAN significantly improves upon SCAN and is the most accurate functional out of the 4 throughout. Similar to ISI-type ACM functionals, nLanE is free from one-electron self-interaction error and thereby reproduces the dissociation of H₂⁺ nearly exactly. Due to the two exact constraints from the weak correlation limit (eq. 6, 8), nLanE-SCAN also has reduced delocalization errors in general as apparent from the improvement over SCAN for the dissociation of He₂⁺. In the strongly correlated closed-shell cases of H₂ and N₂, the HOMO-LUMO gap closes which causes the MP2 correlation energy (eq. 9) to diverge thereby making the linear double hybrid B2PLYP diverge as well. nLanE uses MP2 correlation energy as well but only for the calculation of the initial slope (eq. 8) of the AC, which is modelled through a function (eq. 4) with the correct asymptotic expansion (eq. 5). This is why the

nLanE-SCAN energy does not diverge and also shows improvements over SCAN for these two cases. We expect further improvements through a self-consistent nLanE-SCAN implementation providing it with more accurate orbitals in all cases.

In summary, we have developed a non-linear and non-empirical (nLanE) double hybrid density functional by accurate modelling of the adiabatic connection. Although similar in spirit with other ACM functionals, nLanE-SCAN replaces the explicit constraint from the strongly correlated limit of the AC ($\lambda = \infty$) with the physical fully interacting limit ($\lambda = 1$) obtained from the highly accurate SCAN semi-local DFA. As such, nLanE-SCAN incorporates two exact constraints using wavefunction theory from the weak correlation limit while exploiting the SCAN functional at the fully interacting limit. This choice makes it broadly accurate, similar to SCAN, for multiple tasks across general chemical applications (Table I, Figure 2) where other ACM functionals struggle [43] while regular DFAs perform well. By reducing the (delocalization) error from the weak correlation limit of the SCAN functional, nLanE-SCAN leads to improved energetic predictions in almost all of these cases. At the same time, nLanE also preserves the benefits of ACMs to a large extent as it remains stable for bond dissociations, unlike the divergent traditional linear double hybrid functionals, providing even larger improvements over the SCAN functional in these cases (Figure 3). This is likely due to the accurate form of the used interpolating function for the AC with the correct asymptotic expansions; and the relatively accurate estimate from the SCAN functional as nLanE-SCAN does not explicitly incorporate the strong correlation limit, in contrast to regular ACMs. Future work will deal with a combination of both these approaches along with an analysis of the size-consistency error, role of the chosen DFA for the W_1 limit (eq. 8), and the role of the input orbitals.

I am highly grateful to Prof. Szymon Śmiga and my supervisor Prof. Anatole von Lilienfeld for their valuable advice, insight and feedback on this work. I thank Simon Krug for insightful discussions. I acknowledge support from the Vector Institute in form of a graduate research fellowship, and the University of Toronto for resources and other funding.

DATA AND CODE AVAILABILITY

See github.com/dkhan42/nLanE-DH for PySCF [36] based code for performing nLanE calculations with any choice of DFA for the SCF and W_1 limit. A density-fitting based implementation is also available.

Dataset	MAE [kcal/mol]
W4-11	3.70
G2RC	3.90
DIPCS10	2.78
PA26	0.98
SIE4x4	4.62
ALKBDE10	4.25
YBDE18	2.04
NBPRC	2.51
DC13	6.72
BSR36	1.20
DARC	4.43
BH76	3.09
PX13	4.56
BHDIV10	3.37
S22	0.33
S66	0.34
ADIM6	0.45
IDISP	1.19

TABLE II. nLanE-SCAN mean absolute errors (MAE) functional on the GMTKN55 datasets plotted in Figure. 2 above.

APPENDIX

* danishk.khan@mail.utoronto.ca

- [1] K. Burke, Perspective on density functional theory, *J. Chem. Phys.* **136**, 150901 (2012), <https://doi.org/10.1063/1.4704546>.
- [2] J. P. Perdew, My life in science: Lessons for yours?, *The Journal of Chemical Physics* **160** (2024).
- [3] A. D. Becke, Perspective: Fifty years of density-functional theory in chemical physics, *The Journal of chemical physics* **140** (2014).
- [4] D. Langreth and J. Perdew, The exchange-correlation energy of a metallic surface, *Sol. State Commun.* **17**, 1425 (1975).
- [5] O. Gunnarsson and B. I. Lundqvist, Exchange and correlation in atoms, molecules, and solids by the spin-density-functional formalism, *Phys. Rev. B* **13**, 4274 (1976).
- [6] A. Savin, F. Colonna, and R. Pollet, Adiabatic connection approach to density functional theory of electronic systems, *Int. J. Quantum Chem.* **93**, 166 (2003).
- [7] A. D. Becke, Density-functional thermochemistry. iii. the role of exact exchange, *J. Chem. Phys.* **98**, 5648 (1993).
- [8] J. P. Perdew, M. Ernzerhof, and K. Burke, Rationale for mixing exact exchange with density functional approximations, *J. Chem. Phys.* **105**, 9982 (1996).
- [9] E. Fabiano, L. A. Constantin, P. Cortona, and F. Della Sala, Global hybrids from the semiclassical atom theory satisfying the local density linear response, *J. Chem. Theory Comput.* **11**, 122 (2015).
- [10] K. Sharkas, J. Toulouse, and A. Savin, Double-hybrid density-functional theory made rigorous, *J. Chem. Phys.* **134**, 064113 (2011).
- [11] E. Brémont and C. Adamo, Seeking for parameter-free double-hybrid functionals: The pbe0-dh model, *J. Chem. Phys.* **135**, 024106 (2011).
- [12] E. Brémont, I. Ciofini, J. C. Sancho-García, and C. Adamo, Nonempirical double-hybrid functionals: An effective tool for chemists, *Acc. Chem. Res.* **49**, 1503 (2016).
- [13] M. Seidl, J. P. Perdew, and S. Kurth, Simulation of all-order density-functional perturbation theory, using the second order and the strong-correlation limit, *Phys. Rev. Lett.* **84**, 5070 (2000).
- [14] M. Seidl, J. P. Perdew, and S. Kurth, Density functionals for the strong-interaction limit, *Phys. Rev. A* **62**, 012502 (2000).
- [15] P. Gori-Giorgi, G. Vignale, and M. Seidl, Electronic zero-point oscillations in the strong-interaction limit of density functional theory, *J. Chem. Theory Comput.* **5**, 743 (2009).
- [16] Z.-F. Liu and K. Burke, Adiabatic connection in the low-density limit, *Phys. Rev. A* **79**, 064503 (2009).
- [17] M. Ernzerhof, Construction of the adiabatic connection, *Chem. Phys. Lett.* **263**, 499 (1996).
- [18] A. M. Teale, S. Coriani, and T. Helgaker, Accurate calculation and modeling of the adiabatic connection in density functional theory, *J. Chem. Phys.* **132**, 164115 (2010), <https://doi.org/10.1063/1.3380834>.
- [19] A. Görling and M. Levy, Exact kohn-sham scheme based on perturbation theory, *Phys. Rev. A* **50**, 196 (1994).
- [20] M. Seidl, P. Gori-Giorgi, and A. Savin, Strictly correlated electrons in density-functional theory: A general formulation with applications to spherical densities, *Phys. Rev. A* **75**, 042511 (2007).
- [21] M. Seidl, J. P. Perdew, and M. Levy, Strictly correlated electrons in density-functional theory, *Phys. Rev. A* **59**, 51 (1999).
- [22] E. Fabiano, P. Gori-Giorgi, M. Seidl, and F. Della Sala, Interaction-strength interpolation method for main-group chemistry: Benchmarking, limitations, and perspectives, *Journal of Chemical Theory and Computation* **12**, 4885 (2016).
- [23] M. Ernzerhof, Construction of the adiabatic connection, *Chemical physics letters* **263**, 499 (1996).
- [24] Y. Zhang, X. Xu, and W. A. Goddard, Doubly hybrid density functional for accurate descriptions of nonbond interactions, thermochemistry, and thermochemical kinetics, *PNAS* **106**, 4963 (2009), <https://www.pnas.org/doi/pdf/10.1073/pnas.0901093106>.
- [25] J. Sun, A. Ruzsinszky, and J. P. Perdew, Strongly constrained and appropriately normed semilocal density functional, *Physical review letters* **115**, 036402 (2015).
- [26] L. Goerigk, A. Hansen, C. Bauer, S. Ehrlich, A. Najibi, and S. Grimme, A look at the density functional theory zoo with the advanced gmtkn55 database for general main group thermochemistry, kinetics and noncovalent interactions, *Physical Chemistry Chemical Physics* **19**, 32184 (2017).
- [27] R. J. Gdanitz, Accurately solving the electronic schrödinger equation of atoms and molecules using explicitly correlated (r12-) mr-ci: the ground state potential energy curve of n2, *Chemical physics letters* **283**, 253 (1998).

- [28] T. H. Dunning, Gaussian basis sets for use in correlated molecular calculations. i. the atoms boron through neon and hydrogen, *J. Chem. Phys.* **90**, 1007 (1989).
- [29] M. Levy and J. P. Perdew, Hellmann-feynman, virial, and scaling requisites for the exact universal density functionals. shape of the correlation potential and diamagnetic susceptibility for atoms, *Phys. Rev. A* **32**, 2010 (1985).
- [30] M. Seidl, J. P. Perdew, and S. Kurth, Density functionals for the strong-interaction limit, *Phys. Rev. A* **62**, 012502 (2000).
- [31] A. Görling and M. Levy, Correlation-energy functional and its high-density limit obtained from a coupling-constant perturbation expansion, *Phys. Rev. B* **47**, 13105 (1993).
- [32] T. Li, M. Lin, Z. Hu, K. Zheng, G. Vignale, K. Kawaguchi, A. C. Neto, K. S. Novoselov, and S. YAN, D4FT: A deep learning approach to kohn-sham density functional theory, in *The Eleventh International Conference on Learning Representations* (2023).
- [33] P. M. Gill, B. G. Johnson, J. A. Pople, and M. J. Frisch, An investigation of the performance of a hybrid of hartree-fock and density functional theory, *International Journal of Quantum Chemistry* **44**, 319 (1992).
- [34] S. Grimme and F. Neese, Double-hybrid density functional theory for excited electronic states of molecules, *J. Chem. Phys.* **127**, 154116 (2007).
- [35] S. Vuckovic, P. Gori-Giorgi, F. Della Sala, and E. Fabiano, Restoring size consistency of approximate functionals constructed from the adiabatic connection, *J. Phys. Chem. Lett.* (2018).
- [36] Q. Sun, T. C. Berkelbach, N. S. Blunt, G. H. Booth, S. Guo, Z. Li, J. Liu, J. D. McClain, E. R. Sayfutyarova, S. Sharma, *et al.*, Pyscf: the python-based simulations of chemistry framework, *Wiley Interdisciplinary Reviews: Computational Molecular Science* **8**, e1340 (2018).
- [37] F. Weigend and R. Ahlrichs, Balanced basis sets of split valence, triple zeta valence and quadruple zeta valence quality for h to rn: Design and assessment of accuracy, *Phys. Chem. Chem. Phys.* **7**, 3297 (2005).
- [38] N. Mehta and J. M. Martin, Explicitly correlated double-hybrid dft: A comprehensive analysis of the basis set convergence on the gmtkn55 database, *Journal of Chemical Theory and Computation* **18**, 5978 (2022).
- [39] A. Singh, V. B. Kumar, I. Grabowski, and S. Śmiga, Chapter nine - physically meaningful solutions of optimized effective potential equations in a finite basis set within ks-dft framework, in *Polish Quantum Chemistry from Kotos to Now*, Advances in Quantum Chemistry, Vol. 87, edited by M. Musiał and I. Grabowski (Academic Press, 2023) pp. 297–317.
- [40] S. Śmiga, O. Franck, B. Mussard, A. Buksztel, I. Grabowski, E. Luppi, and J. Toulouse, Self-consistent double-hybrid density-functional theory using the optimized-effective-potential method, *J. Chem. Phys.* **145**, 144102 (2016).
- [41] M. Bursch, H. Neugebauer, S. Ehlert, and S. Grimme, Dispersion corrected r2scan based global hybrid functionals: r2scanh, r2scan0, and r2scan50, *The Journal of Chemical Physics* **156** (2022).
- [42] J. W. Furness, A. D. Kaplan, J. Ning, J. P. Perdew, and J. Sun, Accurate and numerically efficient r2scan meta-generalized gradient approximation, *The journal of physical chemistry letters* **11**, 8208 (2020).
- [43] E. Fabiano, P. Gori-Giorgi, M. Seidl, and F. Della Sala, Interaction-strength interpolation method for main-group chemistry: Benchmarking, limitations, and perspectives, *Journal of Chemical Theory and Computation* **12**, 4885 (2016).